

Morphological study of the pterygoid canal in computed tomography scans of a population from Southeast Brazil

Maria Claudia H. Ferreira, Alexandre R. Freire, Beatriz C. Ferreira-Pileggi, Felipe B. Prado, Ana Cláudia Rossi

Department of Biosciences, Anatomy Division, Faculdade de Odontologia de Piracicaba, Universidade Estadual de Campinas (UNICAMP), Piracicaba, São Paulo, Brazil

SUMMARY

The aim of this study was to evaluate the morphology of the pterygoid canal in computed tomography (CT) scans of a southeastern Brazilian population. One hundred CT scans were evaluated, 58 from male skulls and 42 from female skulls. The Mimics 18.0 software (Materialise, NV, Belgium) was used for segmentation of the images from each CT scan in the region corresponding to the sphenoid bone and the pterygopalatine fossa. After segmentation, volume (mm³) and length (mm) were obtained using a specific tool. The types of pterygoid canals were analyzed according to the following criteria: type 1 (pterygoid canal completely within the sphenoid sinus), type 2 (pterygoid canal on the floor of the sphenoid sinus or partially protruding into the sphenoid sinus), and type 3 (pterygoid canal completely embedded in the sphenoid corpus). Descriptive data for continuous variables were presented as mean and standard deviation or median and interquartile range. Two-way ANOVA tests with Tukey's post hoc test were used for analyzing continuous variables comparing

different types within each sex and between sexes (unpaired analyses). A confidence interval of 95% and a significance level of 5% were established for all tests. Statistical analysis was performed using GraphPAD Prism v.10 software (San Diego, CA, USA). The most common configuration of the pterygoid canal was type 2 for both the right and left sides. For both sides of the evaluated skulls, it was observed that type 3 pterygoid canal had a larger volume in both males and females compared to other types. Although not always significant, for all types, the volume and length in males was higher than in females, especially when comparing types 2 and 3. In conclusion, the morphology of the pterygoid canal may vary among individuals of different sexes, particularly in individuals with type 2 and 3 pterygoid canals. The most incident pterygoid canal was type 2.

Key words: Pterygoid canal – Computed tomography – Morphology – Morphometry – Volume

Corresponding author:

Prof. Ana Cláudia Rossi. Department of Biosciences, Anatomy Division, Faculdade de Odontologia de Piracicaba, Universidade Estadual de Campinas (UNICAMP), 901 Limeira Avenue, 13414-903 Piracicaba, São Paulo, Brazil. E-mail: rossianac01@gmail.com

Submitted: June 20, 2024. Accepted: September 24, 2024

<https://doi.org/10.52083/NYMU6240>

INTRODUCTION

The sphenoid bone is a singular bone that comprises part of the base of the skull and contributes to the formation of the floor of the middle cranial fossa. It is closely associated with cranial nerves and parts of the brain and allows the passage of neurovascular structures into and out of the skull through its foramina and canals. It has a bat-like shape and can be divided into a body, lesser wing, greater wing, and pterygoid processes.

The pterygoid processes originate bilaterally from the connection between the body and the greater wing and project downward. They are composed of the medial and lateral pterygoid plates, which are separated by the pterygoid notch. At the inferior aspect of the pterygoid process, the pterygoid canal is located (Jaworek-Troć et al., 2019).

The Vidian canal (pterygoid canal) was described by the Italian physician, surgeon, and anatomist Guido Guidi (Latin: Vidus Vidius). The pterygoid canal transmits the artery, vein, and nerve of the pterygoid and can be observed at the base of the skull, at the anterior border of the foramen lacerum, through the floor of the sphenoidal sinus, to end in the pterygopalatine fossa (Bahşi et al., 2019).

In studying the pterygoid canal, Santana, et al. (2020), observed that the pterygopalatine fossa is an interosseous space of great anato-functional, pathological, and surgical importance. This is due to its location, anatomical relations, and vasculonervous content that favor the spread of tumorous pathologies. In this interosseous space are the maxillary artery and maxillary nerve (foramen rotundum), as well as the pterygopalatine parasympathetic ganglion, from which branches distribute to the nasal and oral cavities, paranasal sinuses, and parts of the orbital and cranial regions, extending to the face. Additionally, they also observed that the posterior wall of the fossa is an important reference for microsurgery and endoscopic surgery, through different access routes, such as transbuccal, transmaxillary, and transnasal.

The pterygoid nerve is formed by preganglionic parasympathetic fibers of the greater petrosal nerve originating from the geniculate ganglion

of the facial nerve, and by sympathetic fibers of the deep petrosal nerve, which originate from the superior cervical ganglion, via the carotid sympathetic plexus. After leaving the pterygoid canal in the pterygopalatine fossa, the pterygoid nerve enters the posterior face of the Meckel ganglion. Vascular constriction in the nasal cavity is performed by sympathetic fibers, while parasympathetic fibers control secretions from the nasal, palatine, pharyngeal, maxillary sinus, and upper oral and labial glands. Omami et al. (2011) believe that the relative imbalance of parasympathetic to sympathetic stimulation of nasal mucosa blood vessels and glands may be the cause of vasomotor rhinitis, one of the treatments introduced in otolaryngological practice being Vidian neurectomy, which involves surgical sectioning of the pterygoid nerve.

Fortes et al. (2008) stated that for the identification and control of the internal carotid artery and the middle cranial fossa, knowledge of the anatomical relations of the pterygoid nerve and the maxillary nerve is essential. Kassam et al. (2005) report that care should be taken during bone removal, as the space between the maxillary nerve and the pterygoid canal narrows into a cone shape to a relatively narrow space separating the two at the depth of the cranial fossa. Mato et al. (2015) observed that the distance between the pterygoid canal and the foramen rotundum is relevant for endonasal approaches to the quadrangular space, which is limited by the horizontal portion of the petrous part of the internal carotid artery inferiorly, the maxillary nerve laterally, the paraclival carotid medially, and the abducens nerve superiorly. Therefore, it is important to know the distances between the pterygoid canal and the foramen rotundum.

The evaluation of the morphology of the pterygoid canal and its relationship with other structures of the craniofacial complex, such as the sphenoid bone and the foramen rotundum, for example, can contribute to the success of surgical procedures performed in this region. Thus, the aim of this study was to evaluate the morphology of the pterygoid canal in computed tomography (CT) scans of a southeastern Brazilian population.

MATERIALS AND METHODS

The present research was analyzed and approved by the Ethics Committee from FOP/UNICAMP (CAAE protocol: 46463421.9.0000.5418).

Sample

The research used 100 computed tomography of cataloged individuals, whose death was dated between 2008 and 2010, and who were exhumed during the period 2013 and 2014. The computed tomographs were from human skulls belonging to the “Professor Dr. Eduardo Daruge” Osteological and Tomographic Biobank at the Piracicaba Dental School of the University of Campinas (UNICAMP).

The tomographic images were obtained using an Aisteion Multislice 4 CT System (Toshiba Medical Systems Corporation - Japan), for the skull protocol: 100 MA, 120KV, with 1mm slices.

The sample was divided into two groups, one for male samples, with 58 computed tomography of male skulls, and another for female samples, with 42 computed tomography of female skulls. The age of the samples ranged from 18 to 100 years in both groups.

Inclusion and exclusion criteria

The inclusion criteria were: computed tomographies of intact skulls without macroscopic deformities, fractures, or any other pathological or surgical alteration were used. Bone remnants were not excluded due to ancestry or age.

The exclusion criteria were: computed tomography of skulls from syndromic individuals or with any anatomical abnormalities in the region of interest, as well as individuals with implants, plates, screws, or any other metallic artifacts near the region were excluded.

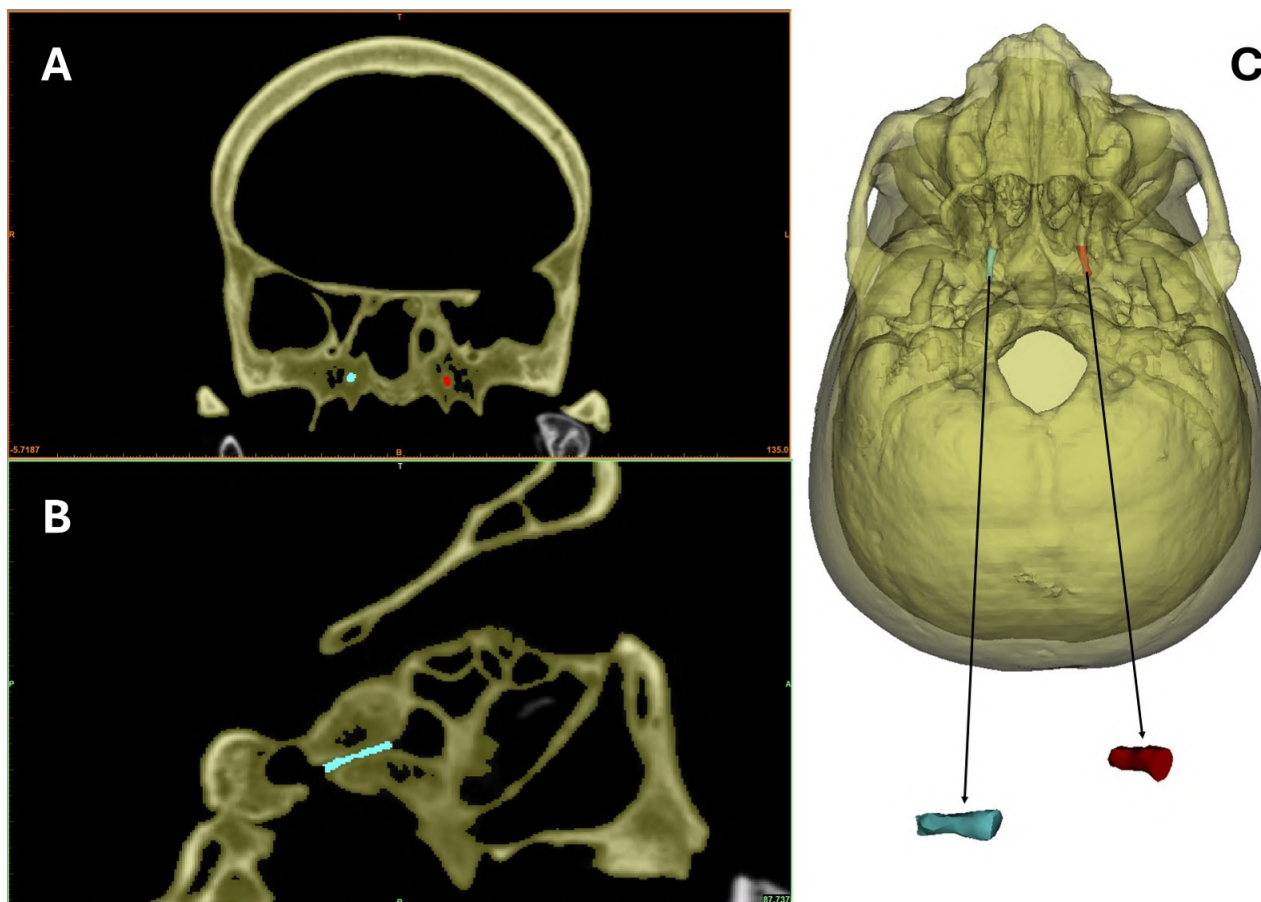


Fig. 1.- CT slices and three-dimensional reconstruction of the human skull highlighting the volume obtained from type 3 pterygoid canal on each side as an example of measurement. **A:** Coronal CT slice showing the right (cyan) and left (red) canals. **B:** Sagittal CT slice showing the right canal (cyan). **C:** Inferior view of three-dimensional reconstruction of skull and pterygoid canals (cyan = right canal, red = left canal) and an isometric projection of the two canals indicated by the arrows. (Mimics 18.0 software - Materialise, NV, Belgium).

Pterygoid Canal Volume and Length evaluation

The Mimics 18.0 software (Materialise, NV, Belgium) was used to perform the segmentation of the images from each computed tomography. Segmentation involved marking each bone structure of interest in each tomographic slice. Segmentation was defined by assessing a threshold to obtain voxels, whose values were established within a range according to the anatomical components evaluated in the corresponding region of the sphenoid bone and pterygopalatine fossa. 3D reconstruction was performed to enable visualization of these components (Fig. 1).

After segmentation, the volume (mm³) and the length (mm) were obtained using a specific tool in the Mimics 18.0 software (Materialise, NV, Belgium). The software calculates the volume from the previously performed segmentation.

Classification of the pterygoid canal

All evaluations were performed using the three-dimensional reconstruction of the computed tomography. The types of pterygoid canal were defined according to Lee et al. (2011):

- Type 1: Pterygoid canal located entirely protruding on the floor of the sphenoid sinus, and one process is present.
- Type 2: Pterygoid canal located partially protruding on the floor of the sphenoid sinus.
- Type 3: Pterygoid canal located entirely within the body of the sphenoid bone.

Statistical analysis

The data were tabulated using the Microsoft Office Excel® package. The analysis of the incidence of morphological types of pterygoid canals was performed using percentages (%). Descriptive data of continuous variables were presented as mean and standard deviation or median and interquartile range. Normality tests were used to assess the distribution of continuous variables. Since the data distribution was normal, the Two-way ANOVA test with Tukey's post-test (unpaired analyses) was used. A confidence interval of 95% and a significance level of deviation of 5% were established for all tests. For multiple comparisons, the initial significance level of 5% was corrected by dividing the initial threshold by the number of comparisons. Statistical analysis was performed using GraphPAD Prism v.10 software (San Diego, CA, USA).

RESULTS

For the evaluated sample, the mean age found was 62.26 (Standard Deviation: 20.80) years for females and 53.86 (Standard Deviation: 17.64) years for males.

Incidence of pterygoid canal types by sex

Out of 100 computed tomographs evaluated, on the right side of the skull, 10% of individuals had type 1 pterygoid canal, 48% had type 2, and 42% had type 3. On the left side, 6% had type 1 pterygoid canal, 54% had type 2, and 40% had type

Table 1. Mean, Standard Deviation, Median, and Interquartile Range of volume (mm³) for comparisons between sexes (male vs. female) in each morphological type found on the right side.

VOLUME (mm ³)	TYPE 1	TYPE 2	TYPE 3
MALE			
Mean	13.38	15.11	23.16
Standard deviation	6.325	9.115	7.630
Median	11.14	12.22	22.91
Interquartile range	16.70	36.36	30.27
FEMALE			
Mean	11.72	12.32	23.00
Standard deviation	5.393	6.863	8.897
Median	11.12	12.53	21.12
Interquartile range	13.00	21.89	28.06

3. When both sides were summed, overall, it was found that 41% of computed tomographs presented type 1 canal, 51% presented type 2, and 8% presented type 3 canal.

When both sides were summed and considering the variable of sex, it was found that for males, 8.7% were type 1, 55.1% were type 2, and 36.2% were type 3. For females, 7.14% were type 1, 45.24% were type 2, and 47.62% were type 3.

Volume (mm³) of pterygoid canal types by sex on each side

Descriptive analysis of Mean, Standard Deviation, Median, and Interquartile Range of volume (mm³) for comparisons between sexes (male vs. female) in each morphological type found on the right side were presented in Table 1.

Assuming normal distribution for both evaluated sides, with alpha=0.05, calculated by the D’Agostino & Pearson test (right side) and Kolmogorov-Smirnov test (left side), the Two-way ANOVA test was performed to assess differences in volume between sexes in each type of pterygoid canal found, and between sides in each type of pterygoid canal found.

The Two-way ANOVA test, for the right side, when comparing volumes of morphological types 1, 2, and 3 between sexes, showed statistically significant differences among types (P <0.0001). On the right side, it was possible to verify that type 3 pterygoid canal had a larger volume for both males and females compared to other types. Although not always significant, for all types, the volume in males was larger than females (P= 0.4643) (Table 1).

Multiple comparisons by Tukey’s test conducted between the means of each morphological type in each sex showed significant differences on the right side when comparing type 2 and type 3 in males (P=0.0075), type 2 and type 3 in females (P=0.0014), type 2 in males with type 3 in females (P=0.0167), and type 3 in males with type 2 in females (P=0.0005) (Fig. 2). No statistical differences were found for other comparisons.

The descriptive analysis of Mean, Standard Deviation, Median, and Interquartile Range of volume (mm³) for comparisons between sexes (male vs. female) in each morphological type found on the left side is presented in Table 2.

The Two-way ANOVA test, for the left side, when comparing volumes of morphological types 1, 2,

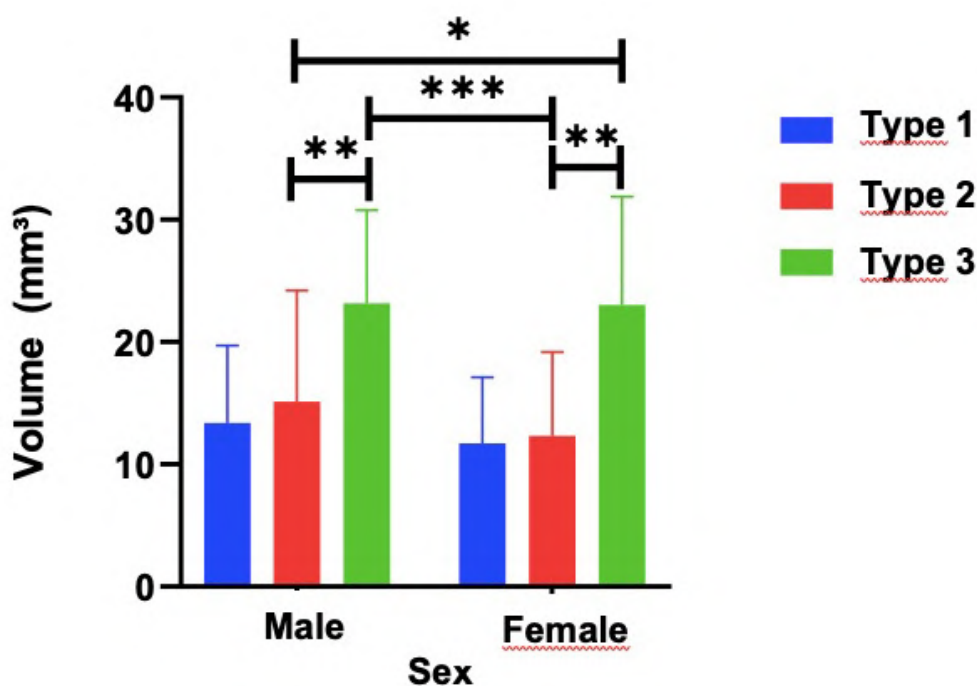


Fig. 2.- Mean volume on the right side (mm³) by sex in each morphological type of pterygoid canal. *Statistical difference.

Table 2. Mean, Standard Deviation, Median, and Interquartile Range of volume (mm³) for comparisons between sexes (male vs. female) in each morphological type found on the left side.

VOLUME (mm ³)	TYPE 1	TYPE 2	TYPE 3
MALE			
Mean	8.945	14.27	24.37
Standard deviation	2.646	13.44	10.92
Median	8.942	11.19	22.88
Interquartile range	5.453	72.48	39.24
FEMALE			
Mean	8.780	9.796	19.67
Standard deviation	3.120	5.256	8.281
Median	8.780	8.764	16.05
Interquartile range	4.413	17.170	24.73

and 3 between sexes, detected statistically significant differences among the types ($P < 0.0001$). On the left side, it was possible to verify that type 3 pterygoid canal had a larger volume for both males and females compared to other types. Although not always significant, for all types, the volume in males was greater than in females ($P = 0.3610$) (Table 2).

Multiple comparisons by Tukey’s test conducted between the means of each morphological type in each sex showed significant differences on the left side when comparing type 2 and type 3 in females

($P = 0.0390$) and type 3 in males with type 2 in females ($P = 0.0034$) (Fig. 3). No statistical differences were found for other comparisons.

Length (mm) of pterygoid canal types by sex on each side

Descriptive analysis of Mean, Standard Deviation, Median, and Interquartile Range of length (mm) for comparisons between sexes (male vs. female) in each morphological type found on the right side were presented in Table 3.

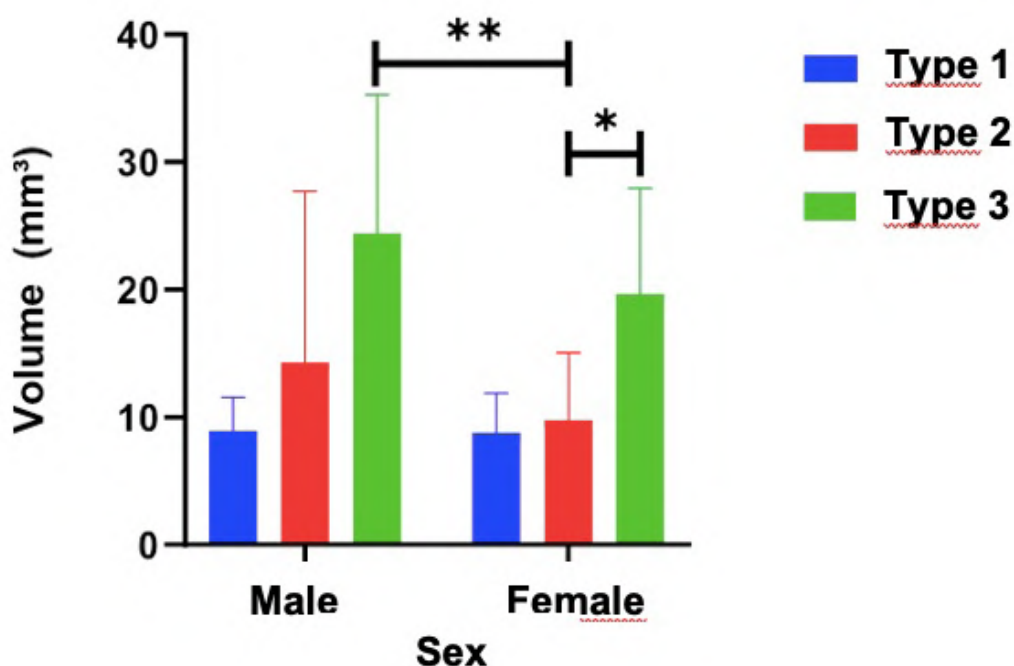


Fig. 3.- Means of volume on the left side (mm³) by sex in each morphological type of pterygoid canal. *Statistical difference.

Table 3. Mean, Standard Deviation, Median, and Interquartile Range of length (mm) for comparisons between sexes (male vs. female) in each morphological type found on the right side.

LENGTH (mm)	TYPE 1	TYPE 2	TYPE 3
MALE			
Mean	11.41	8.887	10.38
Standard deviation	0.8911	3.239	2.006
Median	11.65	9.540	10.36
Interquartile range	2.600	13.33	7.850
FEMALE			
Mean	9.478	7.746	10.16
Standard deviation	1.322	3.457	2.069
Median	9.940	8.140	10.12
Interquartile range	2.950	11.65	7.390

Assuming normal distribution for both evaluated sides, with $\alpha=0.05$, calculated by the D’Agostino & Pearson test (right side) and Kolmogorov-Smirnov test (left side), the Two-way ANOVA test was performed to assess differences in length between sexes in each type of pterygoid canal found and between sides in each type of pterygoid canal found.

The Two-way ANOVA test, for the right side, when comparing length of morphological types 1, 2, and 3 between sexes, showed statistically significant differences among types ($P=0.0021$).

Multiple comparisons by Tukey’s test conducted between the means of each morphological type in each sex showed significant differences on the right side when comparing type 3 in males with type 2 in females ($P=0.0258$) (Fig. 4). No statistical differences were found for other comparisons.

Descriptive analysis of Mean, Standard Deviation, Median, and Interquartile Range of length (mm) for comparisons between sexes (male vs. female) in each morphological type found on the left side were presented in Table 4.

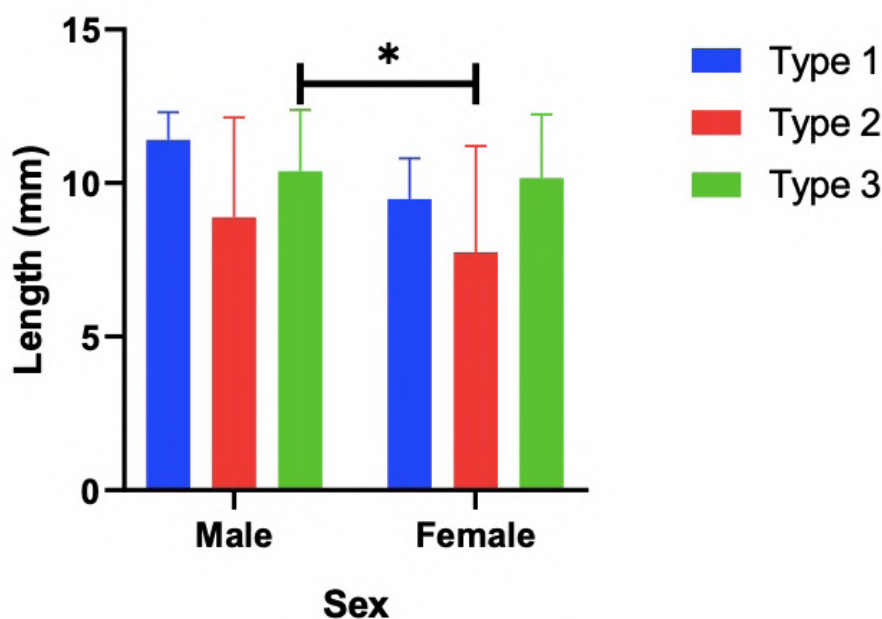


Fig. 4.- Means of length on the right side (mm) by sex in each morphological type of pterygoid canal. *Statistical difference.

Table 4. Mean, Standard Deviation, Median, and Interquartile Range of length (mm) for comparisons between sexes (male vs. female) in each morphological type found on the left side.

LENGTH (mm)	TYPE 1	TYPE 2	TYPE 3
MALE			
Mean	11.76	8.563	10.23
Standard deviation	2.614	3.594	1.619
Median	11.22	9.230	10.16
Interquartile range	6.110	11.74	6.570
FEMALE			
Mean	6.370	7.043	9.739
Standard deviation	3.818	2.755	1.752
Median	6.370	6.410	9.820
Interquartile range	5.400	9.450	6.910

Assuming normal distribution for both evaluated sides, with $\alpha=0.05$, calculated by the D'Agostino & Pearson test (right side) and Kolmogorov-Smirnov test (left side), the Two-way ANOVA test was performed to assess differences in length between sexes in each type of pterygoid canal found and between sides in each type of pterygoid canal found.

The Two-way ANOVA test, for the left side, when comparing length of morphological types 1, 2, and 3 between sexes, showed statistically significant

differences among types ($P=0.0016$) and among sexes ($P=0.0067$).

Multiple comparisons by Tukey's test conducted between the means of each morphological type in each sex showed significant differences on the left side when comparing type 1 in males with type 2 in females ($P=0.0298$), type 3 in males with type 2 in females ($P=0.0077$) and type 2 in female with type 3 in female ($P=0.0317$) (Fig. 5). No statistical differences were found for other comparisons.

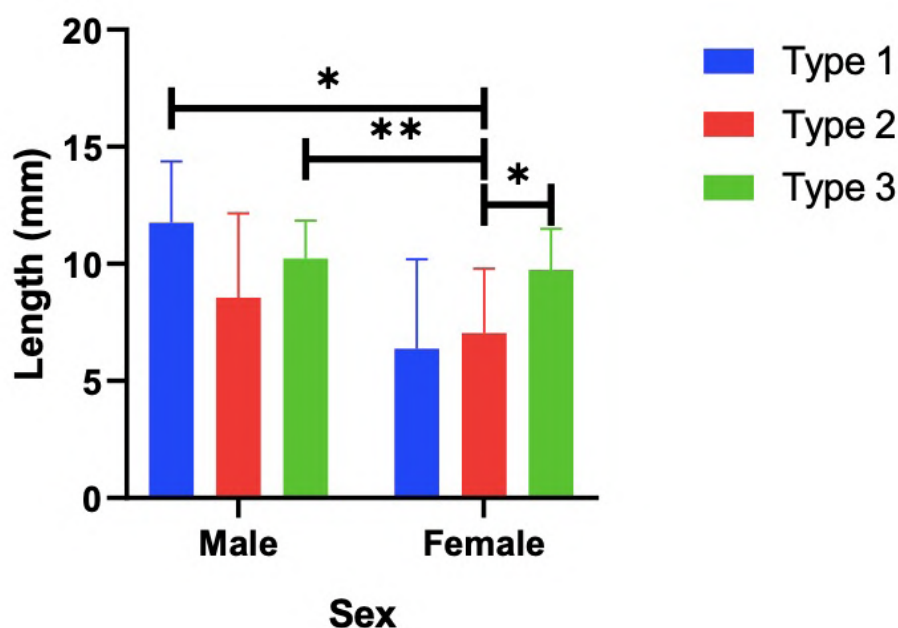


Fig. 5.- Means of length on the left side (mm) by sex in each morphological type of pterygoid canal. *Statistical difference.

DISCUSSION

The pterygoid canal allows the passage of both the nerve and artery of the same name; it lies at the fusion line of the pterygoid process and the greater wing with the body of the sphenoid bone. The pterygoid nerve is formed by the greater petrosal nerve, the deep petrosal nerve, and sympathetic fibers along the internal carotid artery. The pterygoid artery and corresponding nerves pass through the pterygoid canal and are branches of the maxillary artery (Daniels et al., 1998). The pterygoid artery connects parasympathetic fibers to the sphenopalatine ganglion in the pterygopalatine fossa (upper part) (Rypens et al., 1991).

The pterygoid canal may project into the sphenoid sinus and can be affected by sinus diseases and at risk during surgery (Chong et al., 2000). Imaging plays a central role in planning and treating diseases at the skull base because clinical evaluation of this region is often difficult or incomplete. Computed tomography is ideal for delineating bone anatomy and is frequently used (Yazar et al., 2007).

The pterygoid canal is closely related to the sphenoid sinus. Pandolfo et al. (1988) reported that the bone wall between the pterygoid canal and the sphenoid sinus was relatively thin, not exceeding 5 mm, and was incomplete at some points. Therefore, special attention has been given to the morphology and location of the pterygoid canal in relation to the sphenoid sinus during surgery to avoid damage to nerves and blood vessels in the pterygoid canal.

In the present study, the most common configuration of the pterygoid canal was type 2 (partially protruded pterygoid canal on the floor of the sphenoid sinus) for both the right side (48% type 2 canal) and the left side (54% type 2 canal). This is in accordance with Lee et al. (2011), who reported an incidence of 47%. Similarly, Yazar et al. (2007) and Mohebbi et al. (2017) identified type 2 as the most common configuration, with an incidence of 54%. Additionally, they reported cases with bony septum within the pterygoid canal, which likely divides the canal into two parts, nerves, and vessels. Contrary to these reports, Liu et al. (2002) reported more type 3 canal configurations (pterygoid canal entirely located in the body of the sphenoid bone).

To the best of our knowledge, the present study is the first to use volume as a parameter to evaluate the morphology of the pterygoid canal. This serves as critical information for the endoscopic skull base surgeon to use when attempting to safely locate the region.

For both the right and left sides of the evaluated skulls, the Two-way ANOVA test, when comparing the volumes of morphological types 1, 2, and 3 between sexes, showed that the type 3 pterygoid canal had a larger volume for both males and females compared to the other types. Although not always significant, for all types, the volume in males was greater than females, especially when comparing types 2 and 3. Thus, it was observed that sex influenced the volume of the pterygoid canal, and in the pneumatization process, if the sphenoid bone is extensively involved, there is a greater probability of the pterygoid canal projecting into the sinus with a stalk (type 1) or being present on the floor of the sphenoid sinus (type 2) in the sex with larger volume.

The mean length of the pterygoid canal in this present study varies from 6.37 to 11.76 mm. For types 2 and 3, it was possible to verify a significant difference between males and females. In this study, the average length of the pterygoid canal was higher in males than in females, similar to Gong et al. (2023) and Vuksanovic-Bozanic et al. (2019). This may suggest that the pterygoid canal of females is shorter, thicker, and flatter than that of males.

A limitation of the present research is that it was conducted on a specific and regional sample of the population from southeastern Brazil. Therefore, it is important to expand the evaluation to larger samples covering the entire national territory. Nevertheless, this study helps predict the type of pterygoid canal in the Brazilian population.

CONCLUSION

Thus, the results of the present study were in accordance with the hypothesis that the morphology of the pterygoid canal may vary among individuals of different sexes, especially in those who presented pterygoid canals of types 2 and 3. The most prevalent pterygoid canal was type 2.

ACKNOWLEDGEMENTS

The authors sincerely thank those who donated their bodies to science so that anatomical research and teaching could be performed. Results from such research can potentially increase scientific knowledge and can improve patient care. Therefore, these donors and their families deserve our highest respect (Iwanaga et al., 2020). This study was financed in part by the Coordenação de Aperfeiçoamento de Pessoal de Nível Superior – Brasil (CAPES) – Finance Code 001.

REFERENCES

- BAHŞI İ, ORHAN M, KERVANCIOĞLU P, YALÇIN ED (2019) The anatomical and radiological evaluation of the Vidian canal on cone-beam computed tomography images. *Eur Arch Otorhinolaryngol*, 276(5): 1373-1383.
- CHONG VF, FAN YF, LAU DP, CHEE LW, NGUYEN TM, SETHI DS (2000) Imaging the sphenoid sinus: Pictorial essay. *Australas Radiol*, 44: 143-154.
- DANIELS DL, MARK LP, ULMER JL, MAFEE MF, MCDANIEL J, SHAH NC, ERICKSON S, SETHI LA, JARADEH SS (1998) Osseous anatomy of the pterygopalatine fossa. *AJNR*, 19: 1423-1432.
- FORTES FS, SENNES LU, CARRAU RL, BRITO R, RIBAS GC, YASUDA A, RODRIGUES AJ JR, SNYDERMAN CH, KASSAM AB (2008) Endoscopic anatomy of the pterygopalatine fossa and the transpterygoid approach: development of a surgical instruction model. *Laryngoscope*, 118(1): 44-49.
- GONG W, CAO W, ZHANG W, XIANG R, XU Y (2023) Imaging anatomy of the vidian canal and its clinical significance. *Quant Imaging Med Surg*, 13(12): 8704-8728.
- IWANAGA J, SINGH V, OHTSUKA A, HWANG Y, KIM HJ, MORYŚ J, RAVI KS, RIBATTI D, TRAINOR PA, SAŃUDO JR, APAYDIN N, ŞENGÜL G, ALBERTINE KH, WALOCHA JA, LOUKAS M, DUPARC F, PAULSEN F, DEL SOL M, ADDS P, HEGAZY A, TUBBS RS (2020) Acknowledging the use of human cadaveric tissues in research papers. Recommendations from Anatomical Journal Editors. *Clin Anat*, 34: 2-4.
- JAWOREK-TROĆ J, ZARZECKI M, BONCZAR A, KAYTHAMPILLAI LN, RUTOWICZ B, MAZUR M, URBANIAK J, PRZYBYCIEŃ W, PIĄTEK-KOZIEJ K, KUNIEWICZ M, LIPSKI M, KOWALSKI W, SKRZAT J, LOUKAS M, WALOCHA J (2019) Sphenoid bone and its sinus - anatomo-clinical review of the literature including application to FESS. *Folia Med Cracov*, 59(2): 45-59.
- KASSAM AB, GARDNER P, SNYDERMAN C, MINTZ A, CARRAU R (2005) Expanded endonasal approach: fully endoscopic, completely transnasal approach to the middle third of the clivus, petrous bone, middle cranial fossa, and infratemporal fossa. *Neurosurg Focus*, 19(1): E6.
- LEE JC, KAO CH, HSU CH, LIN YS (2011) Endoscopic transsphenoidal vidian neurectomy. *Eur Arch Otorhinolaryngol*, 268(6): 851-856.
- LIU S, WANG Z, ZHOU B, YANG B, FAN E, LI Y (2002) Related structures of the lateral sphenoid wall anatomy studies in CT and MRI. *Lin Chuang Er Bi Yan Hou Ke Za Zhi*, 16(8): 407-409.
- MATO D, YOKOTA H, HIRONO S, MARTINO J, SAEKI N (2015) The vidian canal: radiological features in Japanese population and clinical implications. *Neurol Med Chir*, 55(1): 71-76.
- MOHEBBIA, RAJAEIH S, SAFDARIAN M, OMIDIAN P (2017) The sphenoid sinus, foramen rotundum and vidian canal: a radiological study of anatomical relationships. *Braz J Otorhinolaryngol*, 83(4): 381-387.
- OMAMI G, HEWAIDI G, MATHEW R (2011) The neglected anatomical and clinical aspects of pterygoid canal: CT scan study. *Surg Radiol Anat*, 33(8): 697-702.
- PANDOLFO I, GAETA M, BLANDINO A, LONGO M, FARANDA C (1988) Perineural spread of nasopharyngeal carcinoma: radiological and CT demonstration. *Eur J Radiol*, 8: 231-235.
- RYPENS R, LEMORT M, DOR P, BALERIAUX D (1991) Vidian metastasis of adenoid cystic carcinoma. *J Neuroradiol*, 18: 286-289.
- SANTANA FFM, SILVEIRA MPM, DIAMANTINO PJS, FARDIM KAC, MANHÃES JÚNIOR LRC, COSTA ALF, SAAVEDRA GSFA, LOPES SLPC (2020) Study of the pterigidal canal (vidian canal) through images of cone beam computer tomography. *Brazilian Dental Science*, 23(3): 1-7.
- VUKSANOVIC-BOZARIC A, VUKCEVIC B, ABRAMOVIC M, VUKCEVIC N, POPOVIC N, RADUNOVIC M (2019) The pterygopalatine fossa: morphometric CT study with clinical implications. *Surg Radiol Anat*, 41: 161-168.
- YAZAR F, CANKAL F, HAHOLU A, KILIÇ C, TEKDEMİR I (2007) CT evaluation of the vidian canal localization. *Clin Anat*, 20(7): 751-754.